Widely Tunable Distributed Bragg Reflectors Integrated into Nanowire Waveguides

Anthony Fu,[1,3] *Hanwei Gao,*[1,3,4] *Petar Petrov,*[1,†] *Peidong Yang*[1,2,3*]

[1]Department of Chemistry, University of California, Berkeley, California 94720, United States

[2]Department of Materials Science and Engineering, University of California, Berkeley, California 94720, United States

[3]Materials Sciences Division, Lawrence Berkeley National Laboratory, Berkeley, California 94720, United States

[4]Department of Physics, Florida State University, Tallahassee, Florida 32306, United States

ABSTRACT

Periodic structures with dimensions on the order of the wavelength of light can tailor and improve the performance of optical components, and they can enable the creation of devices with new functionalities. For example, distributed Bragg reflectors (DBRs), which are created by periodic modulations in a structure's dielectric medium, are essential in dielectric mirrors, vertical cavity surface emitting lasers, fiber Bragg gratings, and single-frequency laser diodes. This work introduces nanoscale DBRs integrated directly into gallium nitride (GaN) nanowire waveguides. Photonic band gaps that are tunable across the visible spectrum are demonstrated by precisely controlling the grating's parameters. Numerical simulations indicate that in-wire DBRs have significantly larger reflection coefficients in comparison with the nanowire's end facet. By comparing the measured spectra with the simulated spectra, the index of refraction of the GaN nanowire waveguides was extracted to facilitate the design of photonic coupling structures that are sensitive to phase-matching conditions. This work indicates the potential to design nanowire-based devices with improved performance for optical resonators and optical routing.

KEYWORDS: Distributed Bragg Reflectors, nanowire, photonics, gallium nitride, waveguides, selected-area spectroscopy

Semiconductor nanowires have drawn considerable interest as a platform for miniaturized photonics grown bottom-up.[1-3] Their one-dimensional geometry mimics conventional photonic platforms that use large-aspect-ratio structures such as waveguides and optical cavities in a highly compact geometry. This resemblance has inspired researchers to explore the use of semiconductor nanowires for miniaturized lasers,[4, 5] optical routing,[6, 7] and other optoelectronic components.[8-10] Furthermore, there has been considerable effort in nanowire research to control the size,[11] shape,[12] and composition[13-15] of nanowires for photonic applications. In particular, the ability to manipulate the photonic structure of nanowires has enabled the precise control of their optical properties for improved optoelectronic functions. For example, axially coupling nanowire cavities introduces extra degrees of freedom to manipulate the lasing modes in semiconductor nanowires for single-mode lasing and yields a significant reduction in the lasing threshold at room temperature.[16]

Periodic structures are indispensable for modern optics and optoelectronics. The optical properties of a film can be precisely controlled through careful selection of its material properties and optical structure, which has enabled innumerable inventions in optics and photonics. The integration of periodic structures, such as DBRs,[17, 18] into a nanowire can improve the performance and enable additional photonic functionalities in these compact structures.[19, 20] Previously, there have been reports of embedding nanowires into separate periodic structures to achieve a Purcell enhancement and photonic band gaps in hybrid microresonator structures.[21, 22] Recently, the fabrication of polymer nanofiber-based distributed feedback (DFB) lasers was demonstrated using nano-imprint lithography.[23] The ability to fabricate DBRs in a semiconductor nanostructure is also of considerable interest because inorganic semiconductors generally exhibit favorable transport properties, material stability, and fabrication infrastructure for compact

optoelectronics. Tuned properly, these architectures can be used to select specific wavelengths for optical routing, single-mode lasing, and potentially lower the lasing threshold of nanowire-based lasers.[17, 18] In this work, the integration of DBR structures into GaN nanowires is demonstrated with photonic stopbands that are broadly tunable across the visible spectrum. Numerical simulations based on finite element methods were used to guide the design of the DBR geometry and to analyze the results from the experimental measurements. These DBR-integrated nanowires are promising for compact photonic devices. A method has also been developed to measure the index of refraction of a GaN nanowire waveguide, which can aid in the design of future broadband optoelectronics using building blocks based on nanowires.

DBRs were created by defining periodic indentations in a GaN nanowire using a fabrication scheme based on focused ion beam milling (Figure 1). A detailed description of the fabrication procedure can be found in the Supporting Information. Briefly, single-crystalline GaN nanowires were synthesized via chemical vapor transport using a hot-wall furnace at 900-1000 ^{o}C. These triangularly faceted wires are typically 150-300 nm in cross-sectional height (tip to side facet) and can be up to 150-μm long. A focused ion beam was used to pattern periodic indentations into nanowires with controlled periodicity, duty cycle, and depth of indentation. It is critical to control the alignment and focus of the gallium ion beam and the dosage of milling in order to fabricate these indentations with precise geometric parameters (Figure 1). As demonstrated previously,[16] cut widths as narrow as 30 nm can be achieved. The depth of each cut can be controlled by the beam current and the dosage time down to less than 10 nm. Because the wires are not completely milled through, it is possible to pick up a fabricated wire with a micromanipulator and then transfer it to another substrate for further fabrication or characterization.

Long GaN nanowires (>40 μm) serve as a platform to study DBRs in semiconductor nanowires. In these structures, the periodicity enables large reflection coefficients at the Bragg wavelength due to constructive interference. DBRs with a large number of periods (50-100) and a wide range of periodicities for tunable stopbands can be fabricated into these long nanowires, highlighting this nanoscale integration. Furthermore, for this transmission measurement, a method to normalize the emission that has propagated through the DBR with the emission without the DBR was developed. To account for this normalization, DBRs were fabricated onto one half of the wire while leaving the other half untouched (Figure 2a). When a nanowire is excited with a laser focused at its center, the broad spontaneous emission from defects that has coupled to the waveguide mode will propagate in both directions: through the grating structure and through the un-milled portion of the nanowire (Supporting Information). By selectively collecting the emission from either end of the nanowire, the emission from the DBR end of the nanowire can be normalized by the analyzed emission from the un-milled section of the nanowire.

Selected-area spectroscopy was employed to measure exclusively either the emission that has propagated through the DBR or the emission that has propagated through the unmodified waveguide. A detailed description of the measurement setup and procedure can be found in the Supporting Information. A clear photonic stopband is observed at ~450 nm when the periodicity of the 50 indentations is 143 nm with a cut depth of 40 nm and a cut width of approximately 60 nm (Fig. 2b). This band indicates that the periodic structure efficiently reflects the guided mode at 450 nm. The stopband can blue shift to the UV simply by decreasing the periodicity of the indentations. Furthermore, the measured transmission spectra of various fabricated devices demonstrate a tunable stopband across the visible spectrum from blue to red by increasing the

periodicity and varying the milling conditions in the fabrication process (Figure 2b). The full-width half maximum (FWHM) of these band can be narrow (<5 nm), which can be attributed to the precision in producing repeatable etches over a large number of periods. It is also important to note that by using finite-element methods (COMSOL 4.4a Multiphysics), the optical properties of a DBR in a semiconductor nanowire were investigated from 3D, full-wave simulations, and these simulations were used to predict the position of the stopband. It was found in both the simulation and the measurements that the position of the stopband is most sensitive to the periodicity rather than the cut depth or cut width. A deeper cut depth or wider cut width will blue shift the stopband slightly, which can be understood by examining the Bragg condition from coupled mode theory: $m\lambda_B = 2n_{eff}\Lambda$, where m is the order, λ_B is the Bragg wavelength, n_{eff} is the effective refractive index, and Λ is the grating parameter. A deep or wide cut will lower the effective index of refraction, which will shift the stopband to shorter wavelengths. Furthermore, GaN nanowires have a wide transparency range, and the ability to tune the stopband across a wide range of wavelengths can facilitate the design of broadband optoelectronics for optical routing in a compact geometry.[15, 24, 25] Because the absorption loss varied between each device, the normalized spectrum from the DBR end was divided by the normalized spectrum from the un-milled end to illustrate the tunable stopband. In some cases, less than 30% transmission was observed at the stopband. The ability to spectrally tune the propagation of light across a wide range of wavelengths demonstrates the potential for controllable, wavelength-sensitive optical components with nanometer dimensions for photonic integrated circuits.

Nanowire cavities with integrated DBRs have the potential to be low-threshold nanowire lasers. The naturally cleaved end facets of single nanowires typically exhibit low reflectivity (~20%), which makes these nanowires inefficient resonators (Supporting Information).[16]

Qualitatively consistent with our measured results, finite-element method simulations show that by fabricating DBRs into a nanowire, it is possible to raise the reflectivity at a specific wavelength to over 90% assuming minimal absorption loss (Figure 3). In this case, making many small indentations in the nanowire limits the scattering loss while allowing many small reflections at each indentation to add up in phase and result in a large net reflection at the Bragg wavelength stopband. In lasers, the threshold condition is defined as the point at which the round-trip gain inside a cavity is balanced by the round-trip loss,[18, 26]

$$\Gamma g = \alpha_m + \alpha_p$$

where Γ is the confinement factor, g is the material gain, α_m is the mirror loss, and α_p is the propagation loss. Assuming negligible propagation loss in nanowires because of the shorter cavity length in comparison with conventional edge-emitting semiconductor lasers and the large mirror loss, the laser threshold can be re-written as

$$\Gamma g = \alpha_m = \frac{1}{2L} ln\left(\frac{1}{R_1 R_2}\right)$$

where L is the cavity length and R_1 and R_2 are the reflection coefficients for each end facet, which are nominally equal. The threshold equation shows that this increase in the reflection coefficient achieved in DBR-integrated nanowires can potentially lower the lasing threshold by more than an order of magnitude.

The introduction of a periodic structure into a GaN nanowire can also enable the measurement of the effective index of a waveguide (Figure 4), which further confirms the consistency between the numerical calculations and the experimental results. In materials with anisotropic crystal structures that exhibit birefringence, the bulk refractive index depends on the

polarization of light. In GaN nanowires with triangular cross-sections that grow along the $< 11\bar{2}0 >$ direction (Figure 4a),[27] the exclusive use of the ordinary ray or the extraordinary ray to interpret the effective index of the waveguide is incomplete. A more accurate measurement of the effective index can facilitate improved nanoscale optical design. For example, the evanescent coupling between a resonator and a waveguide is sensitive to the phase-matching condition between the two optical structures.[28, 29] An inaccurate description of the effective waveguide index can potentially lead to overcoupling or undercoupling, where both can limit the degree of coupling efficiency due to mismatched photon lifetimes. One recent example of measuring the refractive index of a nanoribbon was demonstrated for a CdS nanoribbon from 510 nm to 527 nm.[30]

By taking into account the material dispersion of fused silica,[31] the effective bulk index of GaN and the effective index of the waveguide can be extracted by matching the transmission spectra with the corresponding simulation of the fabricated structure. The critical dimensions of the waveguide and the DBR were measured by scanning electron microscopy (SEM) at multiple angles. The periodicity of the grating structure was obtained by a fast Fourier transform (FFT) of the top-down SEM image of the DBR. By tuning the refractive index of GaN to match the measured Bragg wavelength, the effective bulk index was extracted (Figure 4b). This effective bulk index is specific to the GaN nanowire waveguide with triangular cross-sections and can be used to calculate the effective index of the waveguide. Although there are a number of sources of error, the largest was found in the measurement of the FFT pattern. The error bars are calculated by taking the maximum and the minimum of the measured periodicities and then tuning the refractive index to create the bounds to the measurement (Supporting Information). For comparison, the extraordinary and ordinary refractive indices of GaN from two reports were

plotted with the measured effective bulk indices.[32, 33] As expected, the effective bulk indices are relatively bound between the two extremes of these reported values and in other reports.[34] This result further supports the correspondence between the numerical simulations and the experimental results. This methodology to measure the effective index of the waveguide can potentially serve as a set of principles for the design of future broadband, nanostructured photonics.

In summary, DBR structures were fabricated in GaN nanowires using a simple scheme. These devices can offer a platform to demonstrate additional functionalities in semiconductor nanowire photonics. By tuning the geometry of the DBR, these devices displayed tunable photonic band gaps across the visible spectrum. These wires can potentially serve to improve nanoscale optical routing. It is noted that a periodic deposition of material onto the nanowire instead of milling can potentially minimize optical losses even more. A theoretical study of the stopband shows that the reflection coefficient at the band gap of GaN is large enough to potentially lower the lasing threshold of a semiconductor nanowire by more than an order of magnitude. By combining the numerical simulations with the experimental results, the effective index of a nanowire waveguide can be measured to make improved designs for potential photonic coupling schemes. Furthermore, partially milled DBRs in nanowires can potentially enable the introduction of electrical contacts outside the photonic cavity in order to minimize the metal's effect on the optical cavity for an electrically pumped nanowire laser.

FIGURES

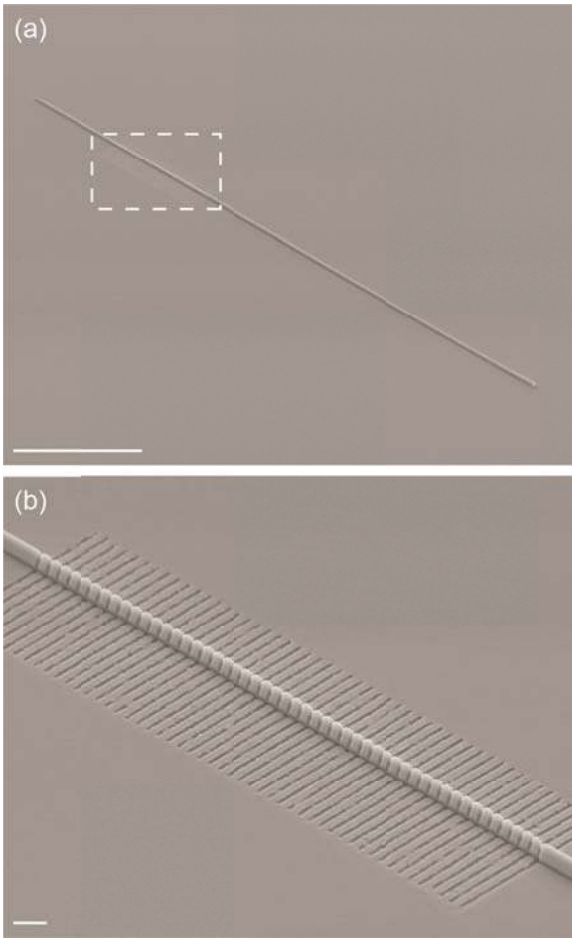

Figure 1. Scanning electron microscopy images of a distributed Bragg reflector fabricated in a GaN nanowire. (a) 45^{o} image of a 54-μm long nanowire with the grating on the top half of the waveguide on a 150-μm thick fused silica substrate with ~1-5 nm of sputtered Au for imaging. Scale bar = 10 μm. (b). Close-up image of (a) showing a 50-period grating with 200-nm periodicity. Scale bar = 1 μm.

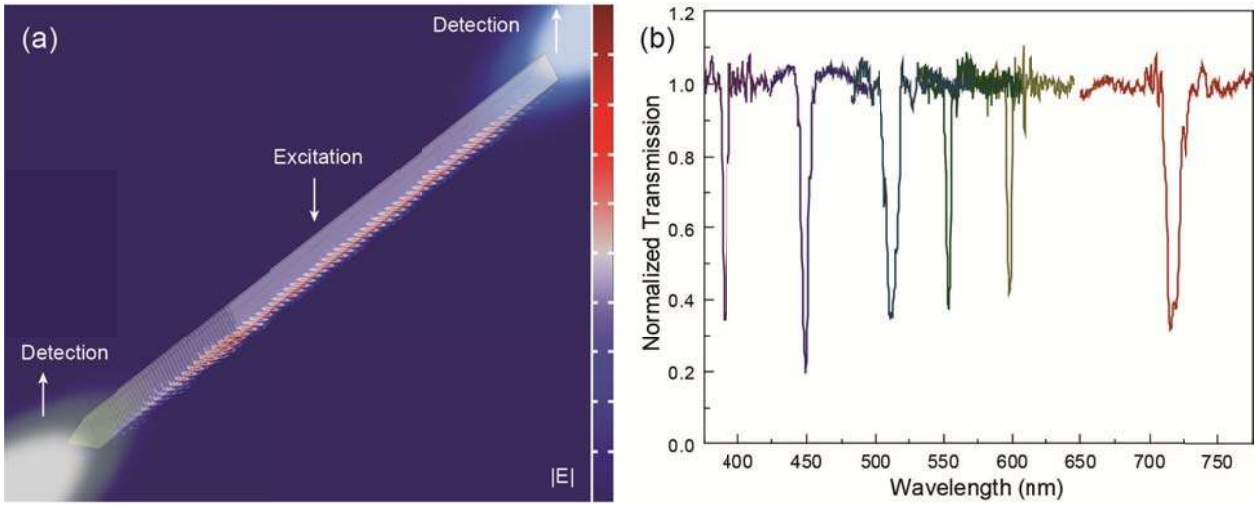

Figure 2. Measurement of the stopbands from DBRs fabricated within a single nanowire. (a) Illustration of the device structure and the measurement of the DBR spectra. The waveguide mode propagates to both ends of the nanowire and the spectra from each end facet are collected separately. The DBR will selectively block the propagation of specific wavelengths. (b) Normalized transmission measurements on six different devices demonstrating tunable photonic band gaps across the visible spectrum for broadband photonics.

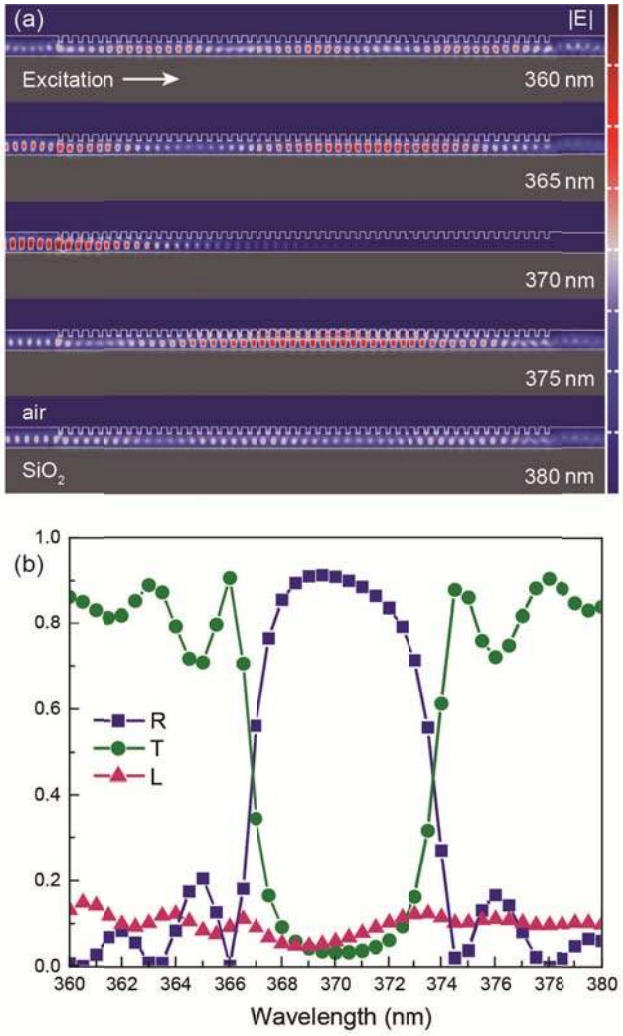

Figure 3. Simulations of the optical properties of a 50-period DBR grating fabricated within a semiconductor nanowire. (a) Electric field maps of various wavelengths propagating from left to right illustrating the wavelength selectivity. At the Bragg wavelength, 370 nm, the field is suppressed and efficiently reflected back. (b). Calculated transmittance, reflectance, and loss as a function of wavelength demonstrating reflection coefficients as high as 90%. The reflectivity of these DBRs implies that the laser threshold of a nanowire laser can be reduced by more than an order of magnitude for improved laser performance.

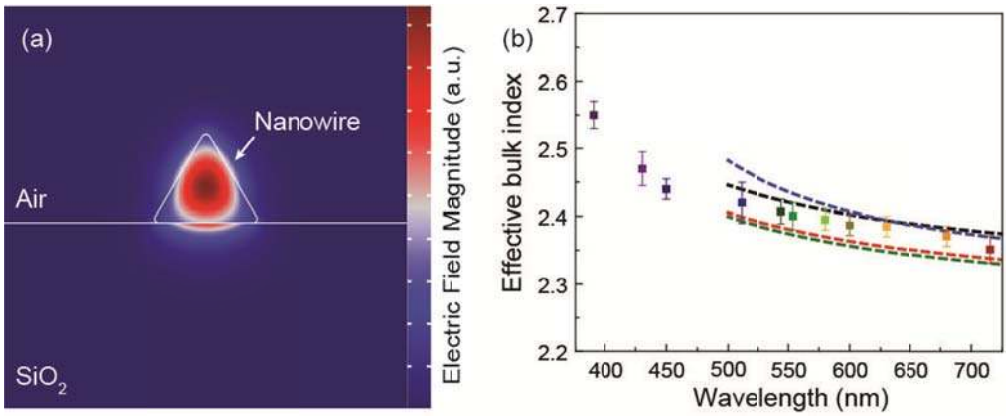

Figure 4. Measurement of the refractive index of a GaN waveguide with a triangular cross-section. (a) Simulated field plot of the fundamental mode of a GaN nanowire waveguide on a fused silica substrate. (b). This simulation geometry was used in conjunction with the measured transmission spectra to calculate the effective bulk index of refraction for a waveguide made from GaN, a material that displays birefringence. The red and green dotted lines and the black and purple dotted lines correspond to the ordinary and extraordinary index of bulk GaN, respectively, from two different literature sources.[32, 33] The measured effective bulk index can help with improving the design for photonic coupling structures that require precise phase-matching conditions.

ASSOCIATED CONTENT

3D full-wave finite element method simulations of both the DBR structure and a single nanowire end facet. Description of the measurement to perform selected-area spectroscopy. Simulation results for nanowires sitting on different facets. Transmission measurement of a fiber-coupled Xe-lamp. Additional SEMs of the fabricated structures. Fast Fourier transforms of the top-down SEM images of the fabricated DBR structures. This material is available free of charge via the Internet at http://pubs.acs.org.

AUTHOR INFORMATION

Corresponding Author

*(P.Y.) E-mail: p_yang@berkeley.edu

Present Addresses

[†]Department of Chemistry, Stanford University, Stanford, California 94305, United States

Author Contributions

A.F., H.G., and P.Y. devised the initial concept. A.F. and P.P. prepared the nanowires and fabricated the devices. A.F. and H.G. performed the optical measurements and designed the numerical calculations. The manuscript was written through contributions of all authors.

Funding Sources

The Office of Science, Office of Basic Energy Sciences of the U.S. Department of Energy under Contract No. DE-AC02—05CH11231.

Notes

The authors declare no competing financial interest.

ACKNOWLEDGMENT

The authors thank Dr. Sarah Brittman for invaluable discussions during the preparation of the manuscript. The authors also thank Dr. Stefano Cabrini, Dr. Simone Sassolini, and Dr. Shaul Aloni for helpful discussions throughout the duration of this work. This work was supported by The Office of Science, Office of Basic Energy Sciences of the U.S. Department of Energy under Contract No. DE-AC02—05CH11231 (P-Chem). This work made use of the imaging and fabrication facilities in the Molecular Foundry at the Lawrence Berkeley National Laboratory, the Marvell Nanofabrication Laboratory at the University of California, Berkeley, and the computing clusters in the Molecular Graphics and Computation Facility at the University of California, Berkeley. A.F. acknowledges the support from the National Science Foundation Center of Integrated Nanomechanical Systems (NSF COINS) under contract No. 0832819.

Insert Table of Contents Graphic and Synopsis Here

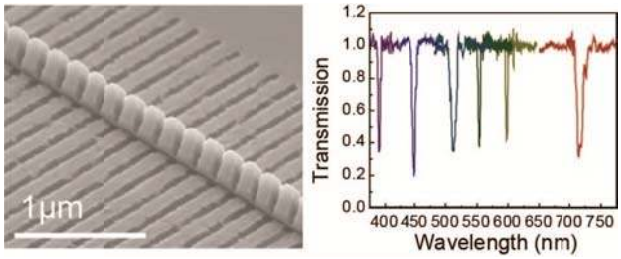

REFERENCES

1. Yan, R.; Gargas, D.; Yang, P., *Nat. Photonics* **2009,** *3*, 569-576.

2. Sirbuly, D. J.; Law, M.; Yan, H.; Yang, P., *J. Phys. Chem. B* **2005,** *109*, 15190-15213.

3. Guo, X.; Ying, Y.; Tong, L., *Acc. Chem. Res.* **2013,** *47*, 656-666.

4. Huang, M. H.; Mao, S.; Feick, H.; Yan, H.; Wu, Y.; Kind, H.; Weber, E.; Russo, R.; Yang, P., *Science* **2001,** *292*, 1897-1899.

5. Saxena, D.; Mokkapati, S.; Parkinson, P.; Jiang, N.; Gao, Q.; Tan, H. H.; Jagadish, C., *Nat. Photonics* **2013,** *7*, 963-968.

6. Law, M.; Sirbuly, D. J.; Johnson, J. C.; Goldberger, J.; Saykally, R. J.; Yang, P., *Science* **2004,** *305*, 1269-1273.

7. Sirbuly, D. J.; Law, M.; Pauzauskie, P.; Yan, H.; Maslov, A. V.; Knutsen, K.; Ning, C.-Z.; Saykally, R. J.; Yang, P., *Proc. Natl. Acad. Sci. U. S. A.* **2005,** *102*, 7800-7805.

8. Greytak, A. B.; Barrelet, C. J.; Li, Y.; Lieber, C. M., *Appl. Phys. Lett.* **2005,** *87*, 151103.

9. Pevec, S.; Donlagic, D., *Appl. Phys. Lett.* **2013,** *102*, 213114.

10. Sirbuly, D. J.; Tao, A.; Law, M.; Fan, R.; Yang, P., *Adv. Mater.* **2007,** *19*, 61-66.

11. Seo, K.; Wober, M.; Steinvurzel, P.; Schonbrun, E.; Dan, Y.; Ellenbogen, T.; Crozier, K. B., *Nano Lett.* **2011,** *11*, 1851-1856.

12. Pauzauskie, P. J.; Sirbuly, D. J.; Yang, P., *Phys. Rev. Lett.* **2006,** *96*, 143903.

13. Pan, A.; Zhou, W.; Leong, E. S. P.; Liu, R.; Chin, A. H.; Zou, B.; Ning, C. Z., *Nano Lett.* **2009,** *9*, 784-788.

14. Qian, F.; Li, Y.; Gradecak, S.; Park, H.-G.; Dong, Y.; Ding, Y.; Wang, Z. L.; Lieber, C. M., *Nat. Mater.* **2008,** *7*, 701-706.

15. Xu, J.; Zhuang, X.; Guo, P.; Zhang, Q.; Huang, W.; Wan, Q.; Hu, W.; Wang, X.; Zhu, X.; Fan, C.; Yang, Z.; Tong, L.; Duan, X.; Pan, A., *Nano Lett.* **2012,** *12*, 5003-5007.

16. Gao, H.; Fu, A.; Andrews, S. C.; Yang, P., *Proc. Natl. Acad. Sci. U. S. A.* **2013,** *110*, 865-869.

17. Chuang, S. L., *Physics of Photonic Devices*. John Wiley & Sons Inc.: Hoboken, NJ, 2009.

18. Coldren, L. A.; Corzine, S. W., *Diode Lasers and Photonic Integrated Circuits*. John Wiley & Sons Inc.: Hoboken, NJ, 1995.

19. Liu, Y.; Meng, C.; Zhang, A. P.; Xiao, Y.; Yu, H.; Tong, L., *Opt. Lett.* **2011,** *36*, 3115-3117.

20. Okazaki, K.; Shimogaki, T.; Palani, I.; Higashihata, M.; Nakamura, D.; Okada, T., Lasing Characteristics of an Optically-Pumped Single ZnO Nanocrystal and Nanomachining for Controlling Oscillation Wavelength. In *ZnO Nanocrystals and Allied Materials*, Springer: 2014, pp 101-123.

21. de Leon, N. P.; Shields, B. J.; Yu, C. L.; Englund, D. E.; Akimov, A. V.; Lukin, M. D.; Park, H., *Phys. Rev. Lett.* **2012,** *108*, 226803.

22. Barrelet, C. J.; Bao, J.; Lončar, M.; Park, H.-G.; Capasso, F.; Lieber, C. M., *Nano Lett.* **2005,** *6*, 11-15.

23. Persano, L.; Camposeo, A.; Carro, P. D.; Fasano, V.; Moffa, M.; Manco, R.; D'Agostino, S.; Pisignano, D., *Adv. Mater.* **2014,** *26*, 6542-6547.

24. Ye, J.; Zhang, C.; Zou, C.-L.; Yan, Y.; Gu, J.; Zhao, Y. S.; Yao, J., *Adv. Mater.* **2014,** *26*, 620-624.

25. Park, H.-G.; Barrelet, C. J.; Wu, Y.; Tian, B.; Qian, F.; Lieber, C. M., *Nat. Photonics* **2008,** *2*, 622-626.

26. Siegman, A. E., *Lasers*. University Science Books: Mill Valley, CA, 1986.

27. Qian, F.; Gradečak, S.; Li, Y.; Wen, C.-Y.; Lieber, C. M., *Nano Lett.* **2005,** *5*, 2287-2291.

28. Haus, H. A., *Waves and Fields in Optoelectronics*. Prentice-Hall: Upper Saddle River, NJ, 1983.

29. Min, B.; Ostby, E.; Sorger, V.; Ulin-Avila, E.; Yang, L.; Zhang, X.; Vahala, K., *Nature* **2009,** *457*, 455-458.

30. Sun, L.; Ren, M.-L.; Liu, W.; Agarwal, R., *Nano Lett.* **2014,** *14*, 6564-6571.

31. Rodney, W. S.; Spindler, R. J., *J. Res. Natl. Bur. Stand.* **1954,** *53*, 185-189.

32. Bowman, S. R.; Brown, C. G.; Brindza, M.; Beadie, G.; Hite, J. K.; Freitas, J. A.; Eddy, C. R.; Meyer, J. R.; Vurgaftman, I., *Opt. Mater. Express* **2014,** *4*, 1287-1296.

33. Chowdhury, A.; Ng, H. M.; Bhardwaj, M.; Weimann, N. G., *Appl. Phys. Lett.* **2003,** *83*, 1077-1079.

34. Bergmann, M. J.; Özgür, Ü.; Casey, H. C.; Everitt, H. O.; Muth, J. F., *Appl. Phys. Lett.* **1999,** *75*, 67-69.